PROCEEDINGS OF SCIENCE

The Plastic Scintillator Detector of the HERD space mission

D. Kyratzis,[*a,b,*] **F. Alemanno,**[†a,b] **C. Altomare,**[c] **F. C. T. Barbato,**[a,b] **P. Bernardini,**[e,f] **I. Cagnoli,**[a,b] **E. Casilli,**[e,f] **P. W. Cattaneo,**[g] **A. Comerma,**[h,i] **I. De Mitri,**[a,b] **F. De Palma,**[e,f] **C. De Vecchi,**[g] **A. Di Giovanni,**[a,b] **M. Di Santo,**[a,b] **A. Espinya,**[h,i] **L. Di Venere,**[c] **M. Fernandez Alonso,**[a,b] **G. Fontanella,**[a,b] **P. Fusco,**[a,b] **F. Gargano,**[c] **D. Gascon,**[h] **E. Ghose,**[e,f,j] **S.Gomez,**[h,i] **D. Guberman,**[h,i] **F. Licciulli,**[c] **F. Loparco,**[c,d] **S. Loporchio,**[c,d] **L. Lorusso,**[c,d] **J. Mauricio,**[h] **M.N. Mazziotta,**[c] **S. Nicotri,**[c] **G. Panzarini,**[c,d] **A. Parenti,**[a,b] **R. Pillera,**[c,d] **A. Rappoldi,**[g] **G. Raselli,**[g] **M. Rossella,**[g] **A. Sammukh,**[h] **A. Sanuy,**[h] **D. Serini,**[c] **I. Siddique,**[a,b] **L. Silveri,**[a,b] **A. Smirnov,**[a,b] **A. Surdo,**[e,f] **R. Triggiani,**[c] **L. Wu**[‡a,b] **for the HERD collaboration**

[a] *Gran Sasso Science Institute (GSSI), Via Iacobucci 2, 67100, L'Aquila, Italy*
[b] *INFN, Laboratori Nazionali del Gran Sasso (LNGS), 67100 Assergi, L'Aquila, Italy*
[c] *Istituto Nazionale di Fisica Nucleare, Sezione di Bari, I-70126 Bari*
[d] *Dipartimento di Fisica "M. Merlin", dell'Università e del Politecnico di Bari, I-70126 Bari, Italy*
[e] *Istituto Nazionale di Fisica Nucleare (INFN)—Sezione di Lecce, Lecce, Italy*
[f] *Dipartimento di Matematica e Fisica "Ennio de Giorgi", Università del Salento, I-73100, Lecce, Italy*
[g] *Istituto Nazionale di Fisica Nucleare (INFN)—Sezione di Pavia, I-27100, Pavia, Italy*
[h] *Institute of Cosmos Sciences - University of Barcelona (ICC-UB), 08028 Barcelona, Spain*
[i] *Serra Húnter Fellow, Polytechnic University of Catalonia (UPC), 08034 Barcelona, Spain*
[j] *Università degli studi di Trento, Dipartimento di Fisica, 38123 Povo, Trento, Italy*

E-mail: `dimitrios.kyratzis@gssi.it, dimitrios.kyratzis@unige.ch`

The High Energy cosmic-Radiation Detection (HERD) facility has been proposed as a main space astronomy payload onboard the China Space Station, with the aim of detecting cosmic rays (CRs) up to a few PeV and gamma-rays greater than 100 MeV. The instrument is designed to accept incident particles from its top and four lateral sides. Owing to its pioneering design, more than one order of magnitude increase in geometric acceptance is foreseen, with respect to previous and ongoing cosmic-ray experiments. The Plastic Scintillator Detector (PSD) constitutes an important sub-detector of HERD, particularly aimed towards photon tagging and precise charge measurements of incoming CRs, from protons to iron. Main requirements concerning its design include: high detection efficiency, broad dynamic range and optimal energy/charge resolution. The detector will be equipped with two layers of orthogonally oriented, short scintillator bars with trapezoidal cross-section, readout by Silicon Photomultipliers (SiPMs). In this work, an overview of the PSD project is presented, along with an illustration of its various design and readout aspects.

38th International Cosmic Ray Conference (ICRC2023)
26 July - 3 August, 2023
Nagoya, Japan

[*] Now at: Department of Nuclear and Particle Physics, University of Geneva, CH-1211 Geneva, Switzerland
[†] Now at: Dipartimento di Matematica e Fisica "Ennio de Giorgi", Università del Salento, Lecce, Italy
[‡] Now at: Institute of Deep Space Sciences, Deep Space Exploration Laboratory, Hefei 230026, China
[*] Speaker

PoS(ICRC2023)140

1. Introduction

Cosmic Ray (CR) studies comprise a significant part of rigorous research activities, with fundamental open questions concerning their origin, acceleration and propagation mechanisms in the Galaxy. Substantial insight arises from the investigation of CRs; originating from violent stellar phenomena, then accelerated to high energies with their subsequent propagation in the Universe, these cosmic messengers provide a unique opportunity for understanding the microscopic world with its intrinsic interactions, as well as the macroscopic world from the perspective of astrophysics/cosmology at the largest scales [1].

Highly–energetic particles were customarily detected only via indirect CR experiments, although with fundamental difficulties in making composition studies with small systematic uncertainties. On the other hand, direct CR experiments provide precise energy and charge measurements of incident particles with small systematics. However, due to rapidly decreasing CR fluxes with energy (and in conjunction with limited exposure), they are limited to statistically-meaningful observations in the multi-TeV range.

Forthcoming space–borne experiments should combine an increased geometric factor (> m^2sr), with extended mission duration (≥10 yr), along with high discrimination power in separating different cosmic radiation components. Therefore, an overall enhancement in detector exposure can be attained, allowing for a deeper understanding of distinctive structures in CR spectra up to the highest achievable energies. In this context, the main objective would be to reach the "knee" in CRs with direct measurements and possibly distinguish the individual "knees" of consecutive elements, thus acquiring valuable information on the maximum energy attained by CR accelerators.

2. The HERD detector

The High Energy cosmic-Radiation Detection (HERD) [2, 3] facility is designed to address the aforementioned requirements, as one of the prominent instruments to be installed on–board the China Space Station (CSS), with a projected duration of more than 10 years. HERD will be capable of directly studying features in the spectra CR nuclei with optimal precision, up to enegies of a few PeV, while also providing insights on various topics concerning: gamma ray astronomy (energies larger than 100 MeV); the electron+positron spectrum and its fine structure up to tens of TeV, while searching for possible signatures of dark matter (DM) annihilation or decay products, owing to its wide Field–of–View (FoV).

HERD, as illustrated in Fig. 1, is designed around a segmented, 3−D imaging calorimeter (CALO). Such a design enables the detection of particles impinging from its top and four lateral sides, as well as precise energy measurements and separation of electrons/protons. A Fiber Tracker (FIT) is situated on all active sides around the calorimeter, in order to accurately determine the incoming direction of primary particles. A Plastic Scintillator Detector (PSD) is enveloping the calorimeter and tracker, aiming to provide gamma–ray and charged particle triggers, together with an essential charge measurement. An additional measurement of the charge will be provided by the Silicon Charge Detector (SCD), covering all sub-detectors mentioned previously. Finally, in order to provide a calibration of the instrument response to nuclei in the TeV region, a Transition Radiation Detector (TRD) is placed on one of HERD's lateral faces.

Consequently, an order of magnitude increase in acceptance can be obtained by a novel design with advanced detector techniques fulfilling all physics requirements, while maintaining a manageable payload for a space mission. The HERD initiative is structured around an international collaboration involving researchers, institutes and universities from China, Italy, Switzerland and Spain contributing to this endeavor.

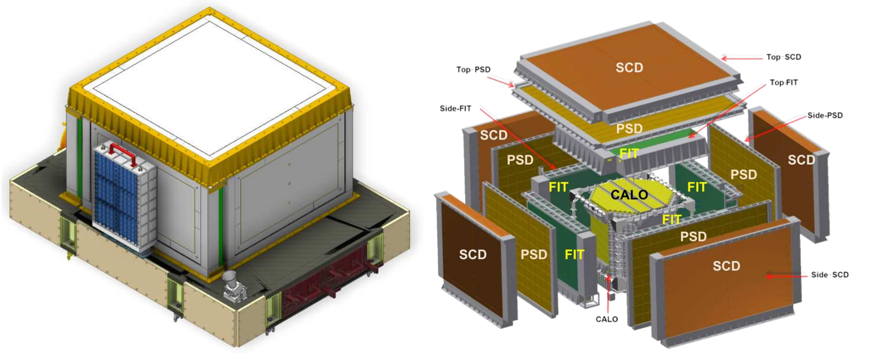

(a) (b)

Figure 1: Representation of HERD, (a) in its complete design, along with (b) an exploded view of the various sub-detectors [3].

3. The Plastic Scintillator Detector

The HERD PSD [4, 5] envelops both CALO and FIT sub-detectors and will discriminate incident photons from charged particles, while providing an essential charge measurement of incoming cosmic–ray nuclei in a range of $Z = 1 - 26$. A schematic view of the proposed PSD instrumentation is viewed in Fig. 2.

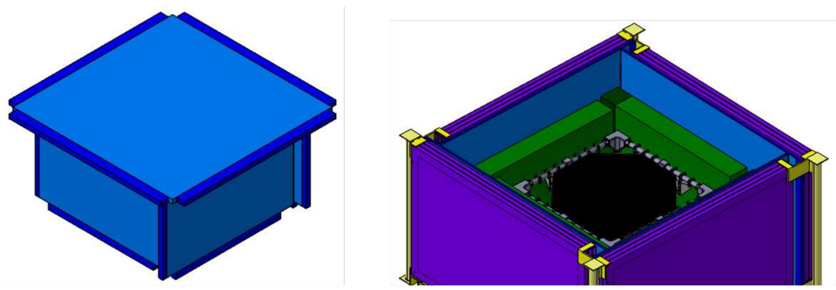

Figure 2: Schematic view of the PSD CAD model illustrating the positioning of the instrumented planes along with its interconnection amongst sub-detectors.

Main requirements concerning the PSD design, include: high detection efficiency, broad dynamic range and good energy resolution. In order to accomplish such objectives, a few different design layouts are currently under consideration, based primarily on the plastic scintillator geometry and number of readout channels. Consequently, the layouts under test involve: long scintillator bars ($159{\times}3{\times}0.5$ cm^3 and $93.3{\times}3{\times}0.5$ cm^3 for horizontal and vertical bars respectively), square tiles (10 cm/side and 0.5-1 cm thickness), along with an intermediate solution between the aforementioned choices, including shorter (in length) but wider bars (30×5×0.5 cm^3), serving as a compromise between the benefits and drawbacks of previous layouts. All configurations present advantages and disadvantages, related (among others) to the optimal number of readout channels versus back–splash (or back–scattering) effects[1] [6]. Ongoing tests and optimization efforts are performed in order to define the best scintillator type and size, SiPM model and quantity to be instrumented, along with an overall verification of the PSD configuration, structural robustness and space readiness tests.

4. Results

A multitude of PSD prototypes regarding different scintillator sizes, geometries and SiPM readouts were thoroughly tested, in order to define the optimal PSD layout. Numerous performance aspects were evaluated with CR muons and electrons from ^{90}Sr radioactive sources, along with particle beams within a broad energy range from accelerator tests at CERN (SPS and PS facilities) and CNAO, in Pavia, Italy. A brief overview of the various performance aspects and design optimization efforts is presented in the following.

Effective light attenuation length

Part of this work pertained to the study of the effective light attenuation[2] (Λ_{Eff}) across PSD bars. For reference, the general light attenuation formula [7] is defined as follows:

$$\mathrm{N(x)} = A_1 \cdot \mathrm{e}^{-\frac{\mathrm{x}}{\Lambda_{\mathrm{S}}}} + A_2 \cdot \mathrm{e}^{-\frac{\mathrm{x}}{\Lambda_{\mathrm{L}}}} + y_0 \simeq \mathrm{N}_0 \cdot \mathrm{e}^{-\frac{\mathrm{x}}{\Lambda_{\mathrm{Eff}}}} \tag{1}$$

where Λ_S and Λ_L correspond to short and long attenuation length components, A_1 and A_2 are the amplitudes and y_0 denotes the constant background. For the sake of simplicity, an "effective" light attenuation length (Λ_{Eff}) is approximated from the general equation, using a single exponential function which includes the collective effects of scintillator size, geometry, cross-section, wrapping material and SiPM readout.

CR muon measurements were performed in several positions along the tested element, for the case of bars and tiles different scintillator sizes and SiPMs (placed at both ends of each PSD prototype) [4]. Concerning PSD bars, all measurements were taken with an external trigger imposed by two scintillator bars readout by single Hamamatsu Photomultipliers (PMTs). In order to maximize trigger performance, both bars are situated orthogonally to the bar under test, with one scintillator being placed above and the other below. In this work, the effective attenuation length of two PSD bar prototypes is highlighted, with their respective sizes amounting to $50 \times 3 \times 1$ cm^3 (1 SiPM/side) and $150 \times 5 \times 1$ cm^3 (2 SiPMs/side). An overview of the effective light attenuation behavior with respect to the external trigger position is illustrated in Fig 3. The attenuation effects were found to

[1]A small fraction of secondaries emitted during electromagnetic showers in the calorimeter, will move backwards and eventually reach the PSD. Electron recoils produced via Compton scattering will also act as a veto for incident gammas, thus decreasing the photon detection efficiency.

[2]As a general definition, the light attenuation length refers to the distance over which the scintillation light intensity emitted by the bar decreases by 1/e.

be low enough, since in each tested configuration at least 50 % of the emitted scintillation photons were detected from one bar end to the other, thus displaying good overall performance regardless of bar length (as seen in Tab. 1).

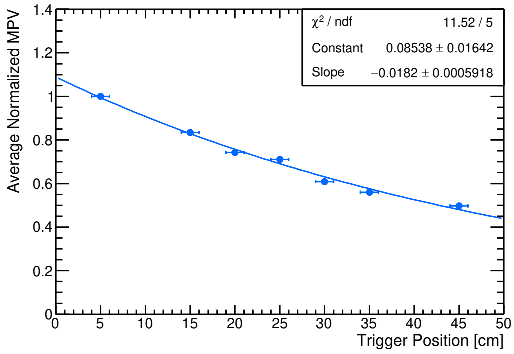

(a)

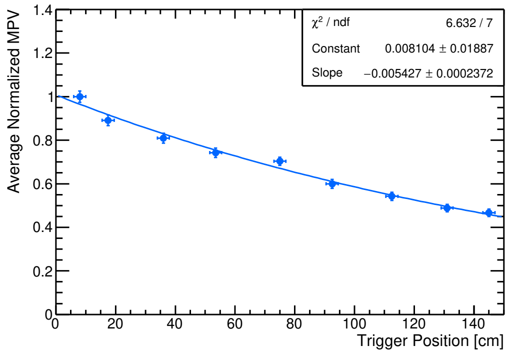

(b)

Figure 3: Normalized Most Probable Values (MPVs) from Landau-convoluted-with-Gauss (LanGaus) fits concerning CR muon measurements, with respect to the external trigger position, where (a) corresponds to a $50 \times 3 \times 1$ cm^3 bar readout by 1 SiPM/side, while (b) shows a $150 \times 5 \times 1$ cm^3 bar readout by 2 SiPMs/side. Both curves are fitted with exponential functions, resulting to effective attenuation lengths of (a) $\Lambda_{\mathrm{Eff}} = 55 \pm 2$ cm and (b) $\Lambda_{\mathrm{Eff}} = 184 \pm 6$ cm, respectively. Both configurations refer to bars of rectangular shape.

Table 1: Measurements' overview for selected PSD bar configurations.

Bar size [cm^3]	Scintillator	SiPM model	Λ_{Eff} [cm]	L-to-R end [%]
$50 \times 3 \times 1$	EJ-200	ASD-NUV3S	55 ± 2	50
$150 \times 5 \times 1$	BC-404	ASD-NUV3S	184 ± 8	49

Beam test activities

All three PSD layouts (short/long bars, tiles) have been successfully validated in numerous beam test campaigns, at the CERN Super Proton Synchrotron (SPS) and Proton Synchrotron (PS) facilities (Figure 4). Concerning the bar prototype, a total of 19 trapezoidal-shaped scintillators (EJ-200 and BC-404) were arranged in two, orthogonally interleaved layers with various wrapping selections. The individual bar dimensions are $50 \times 4 \times 1$ cm^3 (for horizontally-inclined bars) and $50 \times 3 \times 0.5$ cm^3 (for vertically-inclined bars). Regarding the prototype readout, single Printed Circuit Boards (PCBs) were housing 2 Hamamatsu MPPC S14160-3015PS per side (mounted at the respective ends of each bar). The total prototype dimension amounts to 61.4 x 61.4 x 66.8 cm^3. A new, trapezoidal geometry departing from the conventional rectangular cross section has been introduced, in order to address hermeticity issues of adjacent units and impinging event losses. The specific angle selected is 45° (extracted from MC simulations) providing the smallest possible fraction of events lost, in a wide range of impinging particle angles.

For each set of measurements acquired, comparisons between different particle beams (electrons, protons, pions) have been performed at energies of 100 - 350 GeV (electrons and protons) as well as 10 GeV (for pions), along with an overall evaluation of detector response with respect to the beam position. All charge contributions derived from the various beam positions are fitted with LanGaus functions in order to determine the behavior of light propagating through the bars. A complete analysis on vertical and horizontal bars has been performed, according to the collective results of proton, electron and pion beams. The results are shown in Fig. 5, where trapezoidal bars of vertical and horizontal orientation (with different scintillator properties, wrapping, etc) are distinguished in order to provide a clearer picture. All MPVs acquired from their respective fits are normalized to unity. Exponential fits were applied to every curve, with an average value on the effective light attenuation length being measured for the case of horizontal and vertical bars, individually. Following the aforementioned fits, a mean value of all effective attenuation lengths for horizontal and vertical bars alike, amounts to Λ_{Eff} = 45 ± 3 cm and Λ_{Eff} = 43 ± 5 cm, respectively. Evidently, both horizontal and vertical bar geometries are in good agreement, with their effective attenuation length corresponding to their respective bar length.

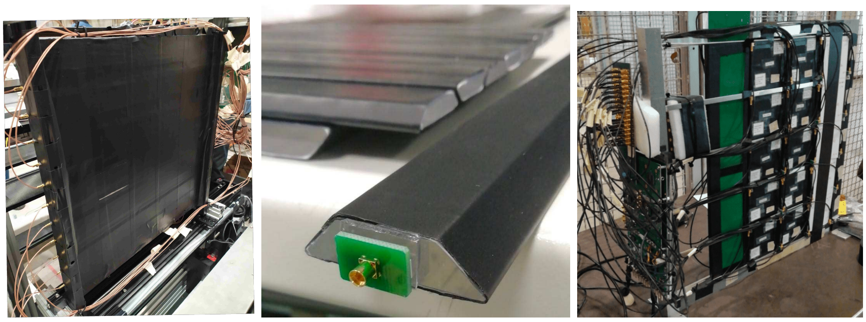

(a) (b) (c)

Figure 4: PSD configurations tested at CERN SPS and PS, with varying particle beams in a wide range of energies. Specifically, (a) corresponds to a bar prototype comprising 19 bars (50 cm in length, 0.5 - 1 cm in thickness) of trapezoidal cross-section (45^o angle), with a readout of 2 SiPMs/side. The bars are divided in two, orthogonally-placed layers. (b) Construction of a single bar readout with 2 SiPMs/side. (c) Prototype consisting of 20 plastic tiles in an array of 4×5 elements (of $10 \times 10 \times 0.5$ cm^3 dimensions each). An individual tile is readout by two PCB boards, each housing 3 SiPMs. From [3].

Another PSD prototype is composed of 8 BC-404 scintillator bars of trapezoidal geometry consisting of two different lengths (40 cm and 30 cm). Each bar is equipped with Hamamatsu 1.3 x 1.3 mm^2 (model S14160-1315) and 3 x 3 mm^2 (model S14160-3015) SiPMs, installed on 2 PCBs (including 3 SiPMs each) connected in parallel, with the addition of 2 SiPMs on the bar ends. The prototype was irradiated with an ion beam of 330 GeV/Z in momentum at CERN SPS, deriving from a primary lead beam of 150 GeV/A in energy, impinging onto a beryllium target with a size of 4 cm and an ion selection of A/Z = 2.2. In the case of decreased energy deposition, the number of scintillation photons increases linearly with regard to primary energy deposition, while for higher energies saturation effects are customarily observed, being well described by Birks' law [8]. As a result, Fig. 6, corresponds to the mean ADC yield with respect to Z^2 of the various primary ions fragmented from the primary lead beam. The aforementioned results stem from the spectral comparison of a given PCB (regarding a bar under test) with a beam-monitoring tile. The halo-core Birks' formula [9] is used to describe the obtained data, leading to a good agreement.

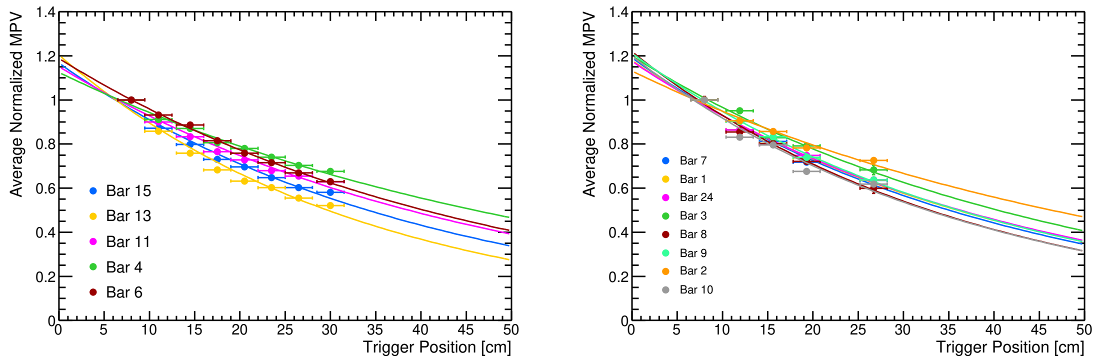

(a) Results on horizontally-inclined bars (b) Results on vertically-inclined bars

Figure 5: PSD prototype tested at CERN SPS and PS. Both figures correspond to normalized MPVs with respect to the particle beam position for the case of (a) horizontally-inclined and (b) vertically-inclined bars, amounting to a total of 13 modules tested. Colored lines correspond to exponential fits, extrapolated to the full length of each bar. Proton and electron beams in a range of 150 - 350 GeV were used in SPS, while pion beam of 10 GeV were utilized in PS.

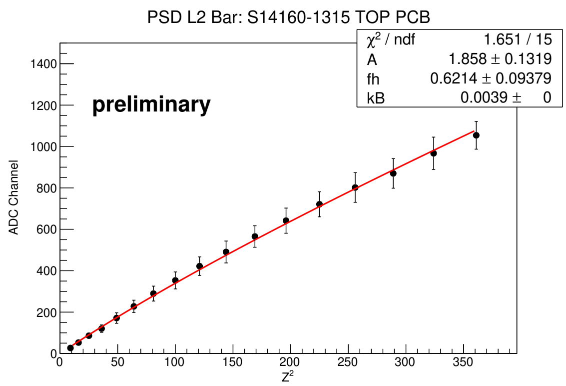

Figure 6: Mean ADC channels as a function of Z^2 of the various primary ions from the selected signals of a PSD module. The red line represents the best-fit obtained using the halo-core Birks' formula [9]. From [10].

5. Conclusion

This work is associated to the design and optimization of the Plastic Scintillator Detector for the HERD space mission. The examined layouts correspond to scintillator prototypes of various sizes and geometries, readout by a number of versatile SiPMs. Part of this work pertained to the study of the effective light propagation across PSD bars, coupled with hermeticity studies that led to a novel instrumentation of trapezoidal PSD configurations (as opposed to the conventional, rectangular cross section) in various sizes. Performance aspects such as attenuation effects (for PSD bar prototypes) were found to be low enough, since in each tested configuration at least 50% of the emitted scintillation photons were detected from one bar end to the other. The effective light attenuation has been consistently similar to the length of each tested bar, thus ensuring an optimal scintillator selection. Additionally, the newly-introduced trapezoidal geometry should be considered towards the PSD realization since it established exceptional hermeticity between all PSD layouts and minimal event losses when charged radiation interacts with the detector under a given angle. As for the recent beam test campaigns, insightful measurements have been realized for the majority of prototype layouts. All PSD configurations yielded good response under a variety of particles (both singly-charged and heavier nuclei) and energies, in conjunction to diverse SiPM models and electronic readouts, hence covering a wide range of performance requirements. As a result, following a spectral analysis of the mean ADC yield with respect to Z^2 of the various primary ions (fragmented from a primary lead beam), a good agreement is evident between the obtained data and the fit from the halo-core Birks formula. Consequently, the proposed PSD configuration will foresee a mechanically robust geometry to sustain vibrations from the launch and prolonged deterioration effects due to radiation damage, as well as fitting all space mission requirements.

Acknowledgements

The author would like to warmly thank all members of the HERD collaboration for the insightful comments and fruitful discussions.

References

[1] R. Aloisio, P. Blasi, I. De Mitri and S. Petrera, *Selected topics in cosmic ray physics*, in *Multiple Messengers and Challenges in Astroparticle Physics*, (Cham), pp. 1–95, Springer International Publishing (2018), DOI.

[2] S.N. Zhang, O. Adriani, S. Albergo, G. Ambrosi et al., *The high energy cosmic-radiation detection (HERD) facility onboard China's Space Station*, *Space Telescopes and Instrumentation 2014 Ultraviolet to Gamma Ray* **9144** (2014) 293 .

[3] D. Kyratzis, *Overview of the HERD space mission*, *Physica Scripta* **97** (2022) 054010.

[4] D. Kyratzis et al., *The Plastic Scintillator Detector of the HERD space mission*, *PoS* **ICRC2021** (2021) 054.

[5] C. Altomare et al., *Status of the plastic scintillator detector for the HERD experiment*, *Nuclear Instruments and Methods in Physics Research Section A: Accelerators, Spectrometers, Detectors and Associated Equipment* (2023) 168237.

[6] A. Moiseev, J. Ormes, R. Hartman, T. Johnson, J. Mitchell and D. Thompson, *Observation and simulations of the backsplash effects in high-energy gamma-ray telescopes containing a massive calorimeter*, *Astroparticle Physics* **22** (2004) 275.

[7] Ł. Kapłon, *Technical attenuation length measurement of plastic scintillator strips for the total-body j-pet scanner*, *IEEE Transactions on Nuclear Science* **67** (2020) 2286.

[8] J. Birks, *Scintillations from organic crystals: Specific fluorescence and relative response to different radiations*, *Proceedings of the Physical Society. Section A* **64** (1951) 874 – 877.

[9] R. Dwyer and D. Zhou, *Plastic scintillator response to relativistic nuclei, z < 28*, *Nuclear Instruments and Methods in Physics Research Section A: Accelerators, Spectrometers, Detectors and Associated Equipment* **242** (1985) 171.

[10] D. Serini et al., *Characterization of the nuclei identification performances of the plastic scintillator detector prototype for the future herd satellite experiment*, in *2023 9th International Workshop on Advances in Sensors and Interfaces (IWASI)*, pp. 184–189, IEEE, 2023.